

CHAPTER ELEVEN

Energy System Alternatives

Part 1. Electromagnetic Principles, Batteries, and Fuel Cells

11.1 Introduction

So far we have considered energy conversion systems that are in widespread use. In this chapter we turn our attention to systems that, to date, have not had major impacts in power generation but appear to have the potential to profoundly influence society within the next few decades.

Most of the preceding study has examined power and propulsion systems that were primarily the outgrowth of thermodynamics and fluid mechanics. We now consider systems among which are several of a fundamentally different character. To better understand these systems, we must invest a little more time in reviewing electromagnetic fundamentals.

In earlier chapters we considered numerous systems that employ the energy conversion chain:

Energy source \Rightarrow Heat \Rightarrow Mechanical energy \Rightarrow Electricity

In this chapter we are concerned with several conversion processes in which the heat-to-mechanical energy transformation link is *not* essential:

Energy source \Rightarrow Electricity

Such processes, in which the source energy is converted directly to electricity, are called *direct energy conversion* processes. While direct energy conversion techniques other than those discussed here exist, we will concentrate on a few that show potential for large-scale power production and that could reach commercialization in the next few decades. Specifically, we focus on fuel cells, solar photovoltaics, and magneto-hydrodynamic systems. In addition, the application of batteries and hydrogen as energy storage media are considered. Let us first develop some principles needed in the analysis of these systems. It would be advantageous for students to relate the fundamental material reviewed in the following sections to chemistry and physics texts with which they are familiar.

11.2 Review of Electromagnetic Principles

A few principles of electromagnetics, fundamental to alternative energy systems, are now reviewed. We will work almost exclusively with SI units in this chapter, except for a few problems framed in the English system.

Charge

A unit of electrical *charge*, q , is the coulomb [C]. The *electron* has a negative charge of 1.6×10^{-19} C and a mass of 9.1×10^{-31} kg. Even the smallest positively charged particle, the proton or hydrogen ion, has a mass more than a thousand times that of the electron. As a result, the electron is much more mobile than neighboring ions and is usually the dominant charge carrier. However, because electromagnetic theory is usually based on the concept of the positive charge, we will think of an electric current as a flow of positive charge, even though motion of electrons in the opposite direction usually transports the charge.

Potential and Field

A positively charged particle influenced by other charged particles may be thought of as being in a force field created by these particles. This field, known as an *electric field*, may be represented by nonintersecting, usually curved surfaces of constant *potential* (V) in three-dimensional space, as sketched in Figure 11.1.

Consider a charged particle located between two potential surfaces of *potential difference* $V_2 - V_1$. A force is exerted on the particle in a direction perpendicular to the local potential surface. The larger the potential difference between the two surfaces, the larger the force. Also, the smaller the distance between surfaces of fixed potential difference, the larger the force. The direction of the force on positively charged particles is from high potential to low, and is oppositely directed for negative particles.

It was indicated that the strength of the force acting on a charged particle between two potential surfaces depends on both the magnitude of $V_2 - V_1$ and how close together the surfaces are. An electric field vector is defined to account for both of these factors. In one dimension, the *electric field intensity* E_x is the negative of the rate of change of potential with respect to distance, $-dV/dx$, the limit of the local potential difference per unit distance in the direction normal to the potential surface. Thus

$$E_x = -dV/dx \approx -\lim (V_2 - V_1)/\delta x \quad [\text{V/m}] \quad (11.1)$$

For a three-dimensional potential field given by $V = V(x, y, z)$, the electric field intensity is a vector, \mathbf{E} (vectors are represented by boldface symbols here) which in terms of Cartesian unit vectors \mathbf{i} , \mathbf{j} , \mathbf{k} is

$$\mathbf{E} = E_x \mathbf{i} + E_y \mathbf{j} + E_z \mathbf{k} \quad [\text{V/m}] \quad (11.2)$$

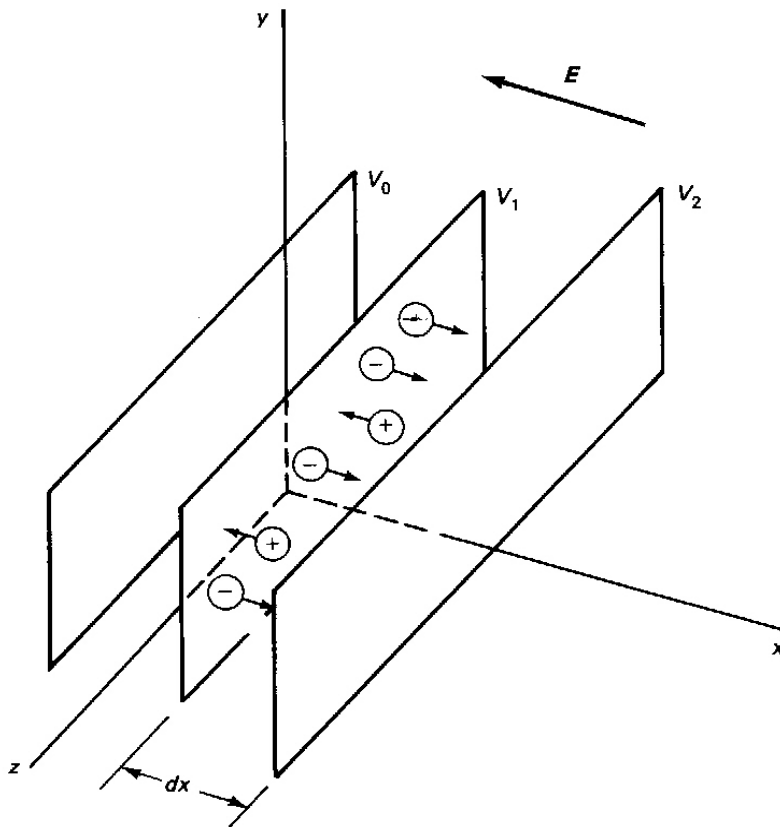


FIGURE 11.1 Surfaces of constant potential in a one-dimensional electric field. $V_2 > V_1 > V_0$.

The electric field vector is related to the potential function $V(x, y, z)$ by

$$\mathbf{E} = -\nabla V(x, y, z) = -(\mathbf{i}\partial V/\partial x + \mathbf{j}\partial V/\partial y + \mathbf{k}\partial V/\partial z) \quad [\text{V/m}] \quad (11.3)$$

where the derivatives in Equation (11.3) are partial derivatives. For a one-dimensional potential, $V = V(x)$, the derivatives with respect to y and z vanish; and the remaining partial derivative becomes the total derivative dV/dx , consistent with Equation (11.1).

The electric field vector gives the magnitude and direction of the force on a positive charge in three-dimensional space. The force on the charge due to the electric field is explicitly represented by the vector equation

$$\mathbf{F} = q\mathbf{E} \quad [\text{N}] \quad (11.4)$$

Equation (11.4) indicates that a force of one newton is exerted on a charge of one coulomb in an electric field of one volt per meter. Hence one coulomb is one newton-meter per volt, or one joule per volt [$1 \text{ C} = 1 \text{ N}\cdot\text{m}/\text{V} = 1 \text{ J}/\text{V}$].

The *work* done to move a positive charge a small distance $d\mathbf{l}$ against the electric field (to a higher potential) is given by the scalar product of the force $-\mathbf{F}$ and the differential distance that the charge moves, $d\mathbf{l} = dx\mathbf{i} + dy\mathbf{j} + dz\mathbf{k}$. Using Equation (11.3), the work is

$$w = -\int \mathbf{F} \cdot d\mathbf{l} = -q \int \mathbf{E} \cdot d\mathbf{l} = q (V_2 - V_1) \quad [\text{C-V}] \quad (11.5)$$

Work is done on the positive charge when the differential distance (dx in Figure 11.1) has a component parallel to the force (and the electric field vector).

Consistent with the observation made in connection with the units of Equation (11.4), Equation (11.5) shows that a coulomb-volt is the same as the usual measure of work, the newton-meter or joule.

When the electric field is specified it becomes unnecessary to think in terms of the associated charge distribution. The electric field may give rise to or resist motions of positive charges or free electrons in the space occupied by the field, just as the original charge distribution would have.

Current and Power

A motion of charges through an electrically conducting medium is called a current. The *current* is the rate at which positive charge passes through a given surface. It is measured in coulombs per second [C/s] or amperes [A]

$$I = dq/dt \quad [\text{A}] \quad (11.6)$$

A current flow produced by an electric field is in the direction of the field and thus is in the direction of decreasing potential, as shown in Figure 11.2. Correspondingly, electrons flow from low to high potential in a direction opposite to the conventional current.

Power is the rate at which work is done. Using Equation (11.5)

$$\text{Power} = dw/dt = Vdq/dt = VI \quad [\text{W}] \quad (11.7)$$

where we now use V for potential difference, as is common. Here it is seen that the unit of power, the watt [W], is the equivalent of the product of amperes and volts [A-V].

Current flows in a medium because of the forces exerted on the charges. For a given potential difference, the current is smaller or larger depending on the ease with which the charges pass through the medium. Thus the current is proportional to the applied potential difference and the *conductance*, G , of the conducting medium. The conductance is usually expressed in terms of its inverse, the *resistance* $R = 1/G$. Resistance is defined by Ohm's Law:

$$R = V/I = 1/G \quad [\Omega] \quad (11.8)$$

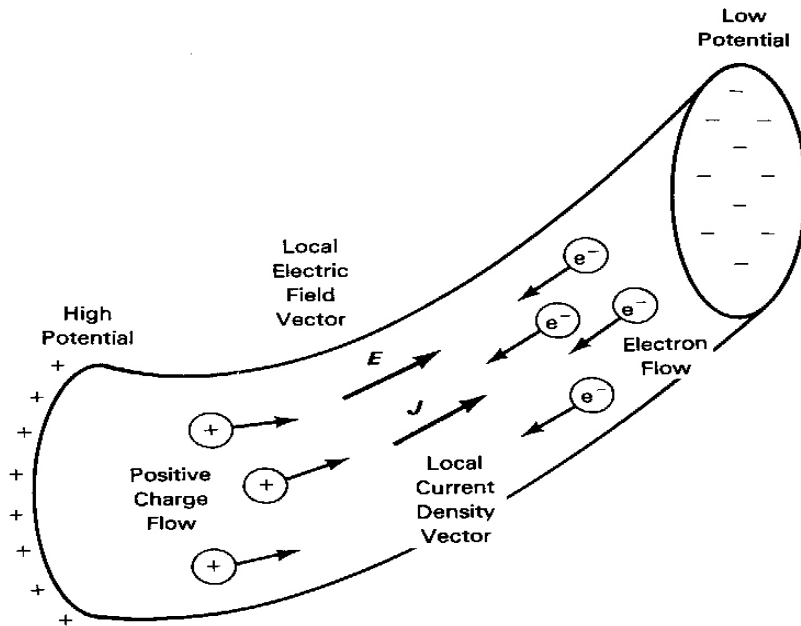


FIGURE 11.2 Flows of current and electrons.

Ohm's Law defines the unit of resistance, the ohm, as the ratio of a volt to an ampere $\Omega = V/A$. Thus the unit of conductance is the inverse ohm or mho Ω^{-1} .

EXAMPLE 11.1

A 12-V battery produces a current of 7 A in a load resistor. Estimate the power delivered to the resistor by the electric field created by the terminals and the magnitude of the resistance. Explain the phenomena in terms of current and electron flow.

Solution

The resistive load has a resistance of $R = V/I = 12 / 7 = 1.71 \Omega$

The power output of the battery is $IV = 7 \times 12 = 84 \text{ W}$.

Current flows from the positive terminal through the load resistor to the negative terminal because of work done by the electric field applied by the battery terminals. In reality, work is done on electrons passing from the negative to the positive terminals. Chemical reactions within the battery provide the energy to move the electrons from the positive to the negative terminals *within* the battery.

The terms *conductance* and *resistance* refer to characteristics of a specific configuration of a conducting material. The terms *electrical conductivity* and *electrical resistivity* refer to intrinsic electrical properties of the material itself. We shall see that the latter properties often are used in dealing with currents in multidimensional fields.

The *current density* \mathbf{J} [A/m^2] is defined as the current per unit cross-sectional area normal to the direction of the current. The electric field vector and the current density are related (Figure 11.2) in a generalized form of Ohm's Law by

$$\mathbf{J} = \sigma \mathbf{E} \quad [\text{A}/\text{m}^2] \quad (11.9)$$

where σ is the *electrical conductivity* of an isotropic conducting medium. In general, when a medium has conductivity varying in direction, the medium is called “anisotropic.” Here we need only consider the isotropic case, where the conductivity of the medium is the same in all directions.

Note that Equation (11.9) indicates that σ must have units of $(\text{A}/\text{m}^2)/(\text{V}/\text{m})$ or $(\Omega\text{-m})^{-1}$. For a cylindrically-shaped conductor, Equation (11.9) may be expressed in terms of the current and potential difference to show that the electrical conductivity is related to the resistance of the conductor by

$$\sigma = J/E = (I/A)/(V/L) = L/(RA) \quad [(\Omega\text{-m})^{-1}] \quad (11.10)$$

where L and A are the length and cross-sectional area of the conductor, respectively. Rewriting Equation (11.10) as $R = L/(A\sigma)$, we see that the resistance of a conductor is proportional to its length and inversely proportional to the electrical conductivity and cross-sectional area, as expected. The *electrical resistivity* ρ [$\Omega\text{-m}$] is the inverse of the electrical conductivity. Thus the resistance of a cylindrical conductor may be written in terms of resistivity as $R = L\rho/A$.

Magnetic Field

We have seen that the electric field may be thought of as representing the effect of a charge distribution on a test charge. Now we turn our attention to a fundamentally different field.

A stationary *magnetic field* exists between the north and south poles of a bar or horseshoe magnet (Figure 11.3). A magnet may be thought of as a collection of tiny magnetic elements, or domains, each having its own north and south poles, which are aligned to produce the magnetic field of the magnet. Magnetic field lines are always closed or terminate on magnetic poles, as opposed to electric field lines, which terminate on charges.

It was observed by Oersted in 1819 that a small magnet deflects when placed in the neighborhood of a wire carrying an electric current. This is explained by the existence of circular magnetic field lines that surround the conductor, as shown in Figure 11.4. Thus not only magnets but electric currents and moving electric charges give rise to

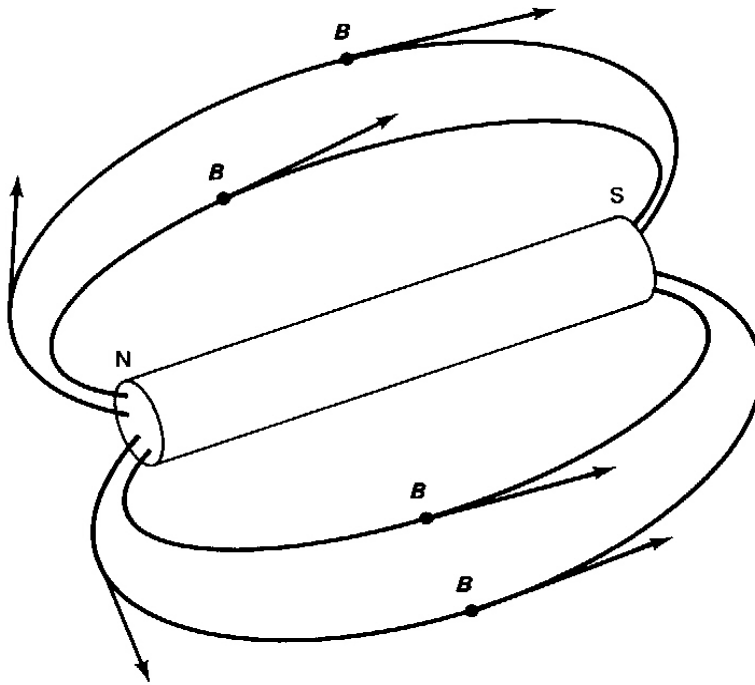


FIGURE 11.3 A bar magnet with local magnetic flux density vectors tangent to the lines of force.

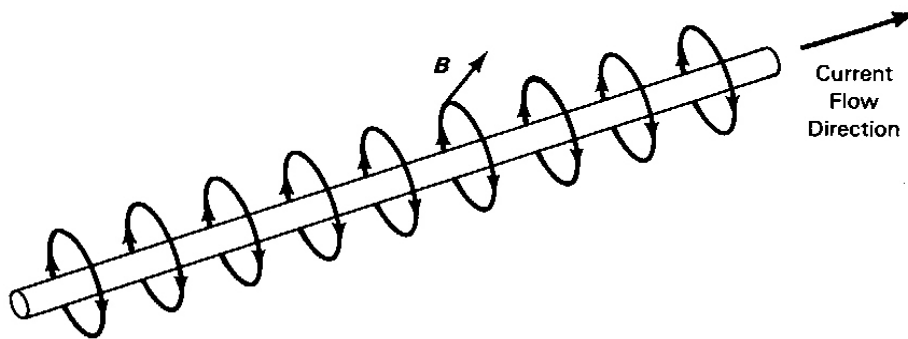


FIGURE 11.4 Magnetic field lines produced by a current-carrying conductor.

magnetic fields. In view of the connection of currents and electric fields, Oersted's discovery indicates that electric fields may produce magnetic fields.

A magnetic field vector \mathbf{B} , called the *magnetic induction* or *magnetic flux density*, is a measure of the strength of a magnetic field and indicates its direction at any point in space (Figures 11.3 and 11.4). Magnetic flux density is measured in webers per square meter [Wb/m^2]. A weber is equivalent to a volt-second. The unit of weber per square meter is also called a tesla.

The magnetic field lines around a circular conductor of electricity are continuous concentric circles, as indicated in Figure 11.4. The direction of the magnetic flux or lines of force around a current carrying conductor is given by the direction of the fingers of the right hand when they are wrapped around it with the thumb pointing in the direction of the current flow.

Twelve years after Oersted observed that electric fields (which produce charge motion, or electric currents) give rise to magnetic fields, Michael Faraday (1831) discovered that magnetic fields can create electric fields. Faraday observed that a current was induced in a stationary circuit by a changing magnetic field produced by a nearby moving magnet. That changing magnetic field could have been created by (1) a *transient current* in a nearby stationary circuit, (2) *motion of a nearby circuit* with a constant current, or (3) *motion of a magnet* in the vicinity. A current, and thus an electric field, is generated in any conductor that experiences a change in its local magnetic field, regardless of whether the observed change is due to the motion of a magnet or to motion of the conductor itself through a stationary magnetic field. The latter phenomenon is the basis of the operation of an electrical generator in which stationary magnets create a current in a rotating armature.

The force exerted on a positive charge in a magnetic field is proportional to the vector product of the charge velocity and the magnetic field strength:

$$\mathbf{F} = q\mathbf{u} \times \mathbf{B} \quad [\text{N}] \quad (11.11)$$

The vector product indicates that charges in a conductor moving with a velocity \mathbf{u} through a magnetic field experience a force in a direction perpendicular to the plane defined by the vectors \mathbf{u} and \mathbf{B} . As indicated in Figure 11.5, the sense of the force is readily determined by rotating the four fingers of the right hand from the velocity vector to the \mathbf{B} vector. The direction of the extended thumb during this operation gives the direction of the force. The force exerted on a coil of an armature of an electric motor is an example of this magnetic action.

In general, both electric and magnetic fields occupy the same space, Thus it is not unusual to speak of a single electromagnetic field represented by the electric and magnetic field vectors. If the electric field intensity is \mathbf{E}' and the magnetic flux density is \mathbf{B} at a given location, the total electromagnetic force acting on a charged particle there, called the *Lorentz force*, is given by

$$\mathbf{F} = q(\mathbf{E}' + \mathbf{u} \times \mathbf{B}) \quad [\text{N}] \quad (11.12)$$

Thus the charge experiences a force that is the vector sum of the electric field vector and a vector perpendicular to both the charge velocity and magnetic flux vectors.

In a coordinate system moving with the velocity \mathbf{u} , the Lorentz force would be given by $\mathbf{F} = q\mathbf{E}$ because the observer in this system sees no motion of the charge. Thus the electromagnetic field felt by the charge may be expressed as an electric field:

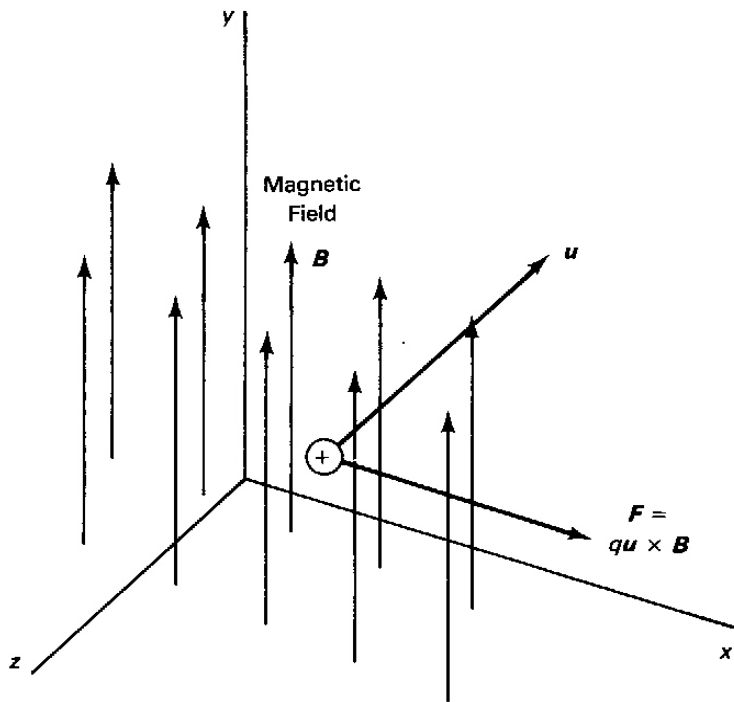


FIGURE 11.5 The force acting on a positive charge moving through a magnetic field.

$$\mathbf{E} = \mathbf{E}' + \mathbf{u} \times \mathbf{B} \quad [\text{N/C}] \quad (11.13)$$

Here \mathbf{E}' is the field existing at the charge location in a stationary coordinate system and \mathbf{E} is the effective electric field sensed by the charge. Thus in a moving coordinate system, the influence of the magnetic field appears as part of the electric field vector.

While our purpose here has been to establish the concepts and relations necessary for an understanding of the energy conversion systems discussed in this chapter, we would be remiss to move on without a few closing comments. We have discussed the interactions of two invisible fields. These spatially varying fields may be thought of as existing in all of space. These are not merely mathematical abstractions but real phenomena. What better proofs of their reality than the electromagnetic waves that a portable radio picks out of space and converts to music to entertain us as we walk or jog, the warmth of solar radiation and the chill of its absence when passing through shade, and the interplanetary signals from space probes that provide amazing views of other planets?

The study of the physics and mathematics of these fields and related phenomena culminated in the formulation of a set of four partial differential equations involving \mathbf{E} and \mathbf{B} that govern electromagnetics. These famous equations known as Maxwell's equations, were firmly established on a consistent basis by James Clerk Maxwell in

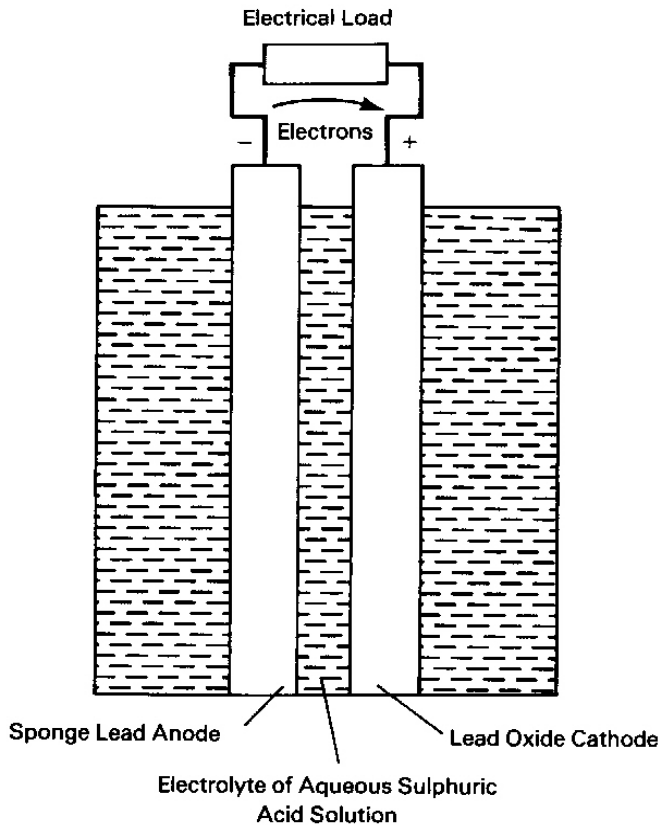


FIGURE 11.6 Diagram of a lead-acid cell.

1860. They mark one of the great triumphs of science because they are capable of quantitatively defining details of countless phenomena in the areas of electricity, magnetism, and radiation. Their use in detailed research and development in energy conversion devices goes well beyond the brief introduction to electromagnetic theory given here. Interested readers may consult, among others, references 6, 26, and 64 for broader and deeper treatments of the subject.

11.3 Batteries and Fuel Cells

Batteries and fuel cells, while structurally and functionally distinct, are based on similar electrochemical principles and technologies. For that reason we have chosen to introduce them together to emphasize their common scientific foundations. They are, however, easily distinguishable, because batteries are devices for the *storage* of electrical energy, while fuel cells are energy *converters* with no inherent energy storage capability. A battery contains a finite amount of chemicals that spontaneously react to produce a flow of electrons when a conducting path is connected to its terminals, as

shown in Figure 11.6. Fuel cells behave similarly, except that chemical reactants are continuously supplied from outside the cell and products are eliminated in continuous, steady streams.

The chemical reactions in batteries and fuel cells are *oxidation-reduction reactions*. A common terminology exists for both types of cells. Both contain electrode pairs in contact with an intervening *electrolyte* (the charge-carrying medium), as in Figure 11.6. The electrolyte is a solution through which positively charged ions pass from the anode to the cathode. The negative electrode, called the *anode*, is where an *oxidation* reaction takes place, delivering electrons to the external circuit. The positive electrode, where *reduction* occurs, is called the *cathode*. Electrons flow through the external load from the negative to the positive electrode, while the conventional current flows in the opposite direction from high to low potential. At the cathode, electrons arriving from the external load are neutralized by reaction with positive ions from the electrolyte.

The use of electrical storage cells dates back to the early 1800s. In 1800, Alessandro Volta gave the first description of an electrochemical cell in a letter to the British Royal Society. The invention of the telegraph in the 1830s provided strong motivation for the development and manufacture of this electrical energy source. Though the electrochemical cell provided electrical energy for the telegraph and other inventions, it would be half a century before central plant electrical power became available. In 1839, Sir William Grove demonstrated the fuel cell concept, but it was not until the 1950s that significant progress was made toward the development of useful fuel cells.

Batteries designed for a single discharge cycle (flashlight batteries, for example) are called *primary cells*; those that can be discharged and recharged numerous times are called *secondary cells*. Fuel cells, on the other hand, utilize chemicals that flow into the cell to provide a more or less continuous supply of direct current. Before considering the exciting possibilities of fuel cells, we will take a brief look at batteries, with emphasis on secondary cells because of their current and future technical importance.

Batteries

Enormous numbers of batteries are used in a variety of applications, from the tiny button cells in wristwatches, to the cells in flashlights, to the starting, lighting, and ignition (SLI) batteries in automobiles, to the large batteries found in submarines for submersed operations, as well as in emergency power supplies, and remote relay stations. Batteries have been considered for some time for load-leveling power plants as alternatives to pumped hydroelectric and compressed-air storage. While batteries have been used as propulsion power sources for road vehicles for about a century (according to ref. 10 an electric car held the world land speed record of 66 mph in 1899), they have not been competitive with the fossil-fueled internal combustion engine. However,

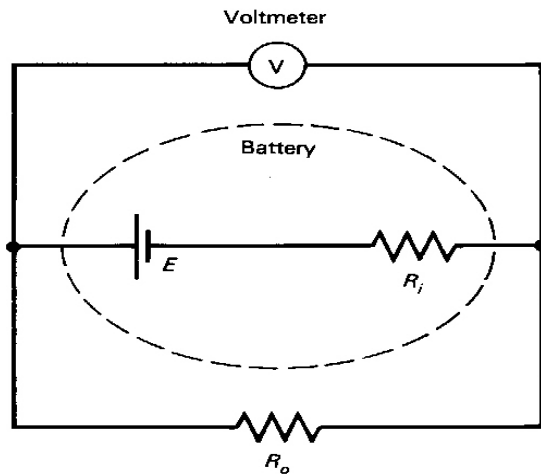


FIGURE 11.7 Circuit diagram for battery model in Example 11.2.

a renewed interest in this application has developed as research in battery technology and the public sensitivity to pollution by internal combustion engine-propelled vehicles has become more advanced.

It has been pointed out that batteries are basically devices for storing charge and automatically delivering an electrical current flow, on demand, for a limited time. A battery consists of one or more cells connected in series to provide a particular open circuit voltage or *electromotive force* (EMF). Each chemical cell typically has an EMF of about two volts, although the exact value is dependent on the specific cell reactants.

A Simple Mathematical Model of a Battery. When current is drawn from a battery, the voltage across its terminals decreases below its EMF, largely due to the internal voltage drop associated with the battery's internal resistance. Thus a simple model of a battery involves a constant voltage source in series with a constant resistance.

Following Figure 11.7, the terminal voltage for this model is given by the difference between the EMF and the internal resistive potential drop:

$$V = E - IR_i \quad [\text{V}] \quad (11.14)$$

and the current is

$$I = E / (R_i + R_o) \quad [\text{A}] \quad (11.15)$$

EXAMPLE 11.2

The voltage of a lead-acid battery with an EMF of 12.7 V is measured as 11.1 V when it delivers a current of 50 amperes to an external resistance. What are the internal and external resistances? What is the battery voltage and the current flow through a 5-Ω resistor? Sketch the voltage–current characteristic.

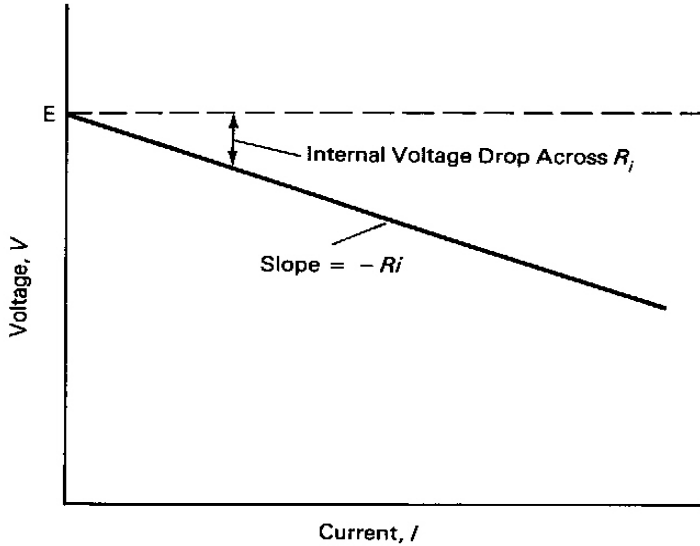


FIGURE 11.8 Voltage–current relation for linear battery model.

Solution

Solving Equation (11.14) for R_i and Equation (11.15) for R_o , we obtain the internal and external resistances:

$$R_i = (E - V)/I = (12.7 - 11.1)/50 = 0.032 \, \Omega$$

$$R_o = E/I - R_i = 12.7/50 - 0.032 = 0.222 \, \Omega$$

With the constant internal resistance established, the current flow through a 5- Ω external resistor is then given by Equation (11.15):

$$I = E/(R_i + R_o) = 12.7/(0.032 + 5) = 2.524 \, \text{A}$$

Note that if R_o were infinite in Equation (11.15), the current would vanish and the cell voltage would be equal to the EMF, as in an open circuit.

The cell voltage with the 5- Ω resistor is given by equation (11.14):

$$V = E - IR_i = 12.7 - 2.524(0.032) = 12.62 \, \text{V}$$

or

$$V = IR_o = 2.524(5) = 12.62 \, \text{V}$$

By Equation (11.14), the voltage characteristic is a straight line (see Figure 11.8) with intercept E and slope $-R_i$.

While the linear model is useful and informative, it does not conform precisely to real battery characteristics. As in the model, real batteries are capable of providing current and power to a wide range of resistances with little voltage drop for short periods of time. However, the model fails for long periods of time and when large currents are drawn, because it does not account for the finite amount of stored chemical energy and reaction rate limitations encountered in real batteries. In these circumstances, the terminal voltage and power output drop drastically as cell chemicals are consumed.

Secondary cell reactions are approximately internally reversible. Thus, by application of an external direct current source, internal battery reactions may be reversed over a period of time in a process called *charging*. In a conventional automotive application, electrical power for lighting, ignition, radio, and so on is supplied by an engine-driven alternator. Normally, the battery is required only for engine starting and to compensate for possible alternator output deficits when the engine runs slowly. A voltage regulator maintains a steady electrical system voltage and controls battery charging when excess alternator current is available and needed. According to reference 27, the regulator limits the charging voltage of a 12-V battery to about 14.4 V.

Battery Performance Parameters. Important parameters characterizing battery performance are the storage capacity, cold-cranking amperes, reserve capacity, energy efficiency, and energy density.

The *storage capacity*, a measure of the total electric charge of the battery, is usually quoted in ampere-hours rather than in coulombs (1 amp-hour = 3600 C). It is an indication of the capability of a battery to deliver a particular current value for a given duration. Thus a battery that can discharge at a rate of 5 A for 20 hours has a capacity of 100 A-hr. Capacity is also sometimes indicated as *energy storage capacity*, in watt-hours.

Cold-cranking-ampereage, CCA, for a battery composed of nominal 2-V cells is the highest current, in amperes, that the battery can deliver for 30 seconds at a temperature of 0°F and still maintain a voltage of 1.2 V per cell (ref. 27). The CCA is commonly used in automotive applications, where the problem of high engine resistance to starting in cold winter conditions is compounded by reduced battery performance. At 0°F the cranking resistance of an automobile engine may be increased more than a factor of two over its starting power requirement at 80°F, while the battery output at the lower temperature is reduced to 40% of its normal output. The reduction in battery output at low temperatures is due to the fact that chemical reaction rates decrease as temperature decreases.

The *reserve capacity* rating is the time, in minutes, that an SLI battery will deliver 25 amperes at 80°F. This is an indication of how long the battery would continue to satisfy essential automotive operating requirements if the alternator were to fail.

Other parameters evaluate batteries with respect to energy for traction or other deep-cycling applications where, in contrast to SLI applications, their state of charge becomes low regularly. The *energy efficiency* is the ratio of the energy delivered by a

fully charged battery to the recharging energy required to restore its original state of charge. For transportation purposes where weight and volume are critical, the *energy density* is an important parameter. It may be represented on a mass basis, in watt-hours per kilogram, or on a volume basis, in watt-hours per cubic meter.

Analysis of a Cell. Consider a reversible cell with a terminal potential difference V discharging with a current I through a variable resistance. The flow of electrons through the load produces the instantaneous electrical power, IV . At low currents the cell voltage is close to the cell EMF and the external work done and power output are small. Suppose that chemical reaction in the battery consumes reactant at an electrode at a rate of n_c moles per second. Electrons released in the reaction flow through the electrode to the external load at a rate proportional to the rate of reaction, jn_c , where j is the number of moles of electrons released per mole of reactants. It will be seen later that, for a lead-acid battery, two moles of electrons are freed to flow through the external load for each mole of lead reacted. Hence, in this case $j = 2$. Thus jn_c is the rate of flow of electrons from the cell, in moles of electrons per second. There are 6.023×10^{23} electrons per gram-mole of electrons, and each has a charge of 1.602×10^{-19} C. Thus the product

$$F = (6.023 \times 10^{23})(1.602 \times 10^{-19}) = 96,488 \text{ C/gram-mole}$$

is the charge transported by a gram-mole of electrons. The constant F is called *Faraday's Constant*, in honor of Michael Faraday, a great pioneer of electrochemistry. The electric current from a cell may then be related to the rate of reaction in the cell as

$$I = jn_c F \quad [\text{A}] \quad (11.16)$$

and the instantaneous power delivered by the cell is:

$$\text{Power} = jn_c F V \quad [\text{W}] \quad (11.17)$$

The cell electrode and electrolyte materials and cell design determine the maximum cell voltage. Equations (11.16) and (11.17) show that the nature and rate of chemical reaction control the cell current and maximum power output of a cell. Moreover, it is clear that the store of consumable battery reactants sets a limit on battery capacity.

Lead-Acid Batteries. By far the most widely used secondary battery is the lead/sulfuric acid/lead oxide ($\text{Pb}/\text{H}_2\text{SO}_4/\text{PbO}_2$), or lead-acid battery, by virtue of its widespread application in automobiles for starting, lighting, and ignition and in

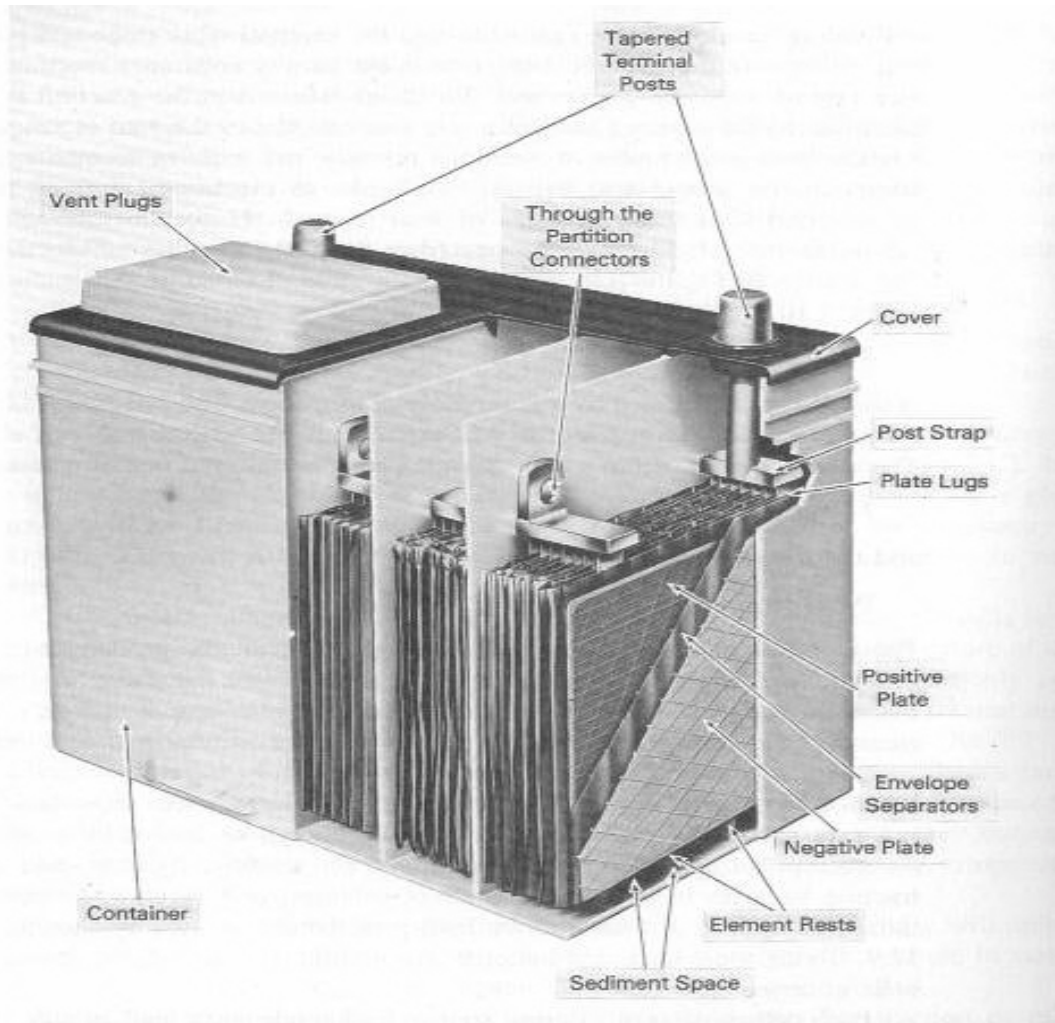


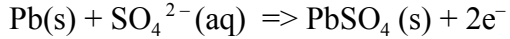
FIGURE 11.9 Cutaway drawing of a lead-acid battery. (Courtesy of Battery Council International.)

traction batteries used in rail and street vehicles, golf carts, and electrically powered industrial trucks. An automotive lead-acid battery is shown schematically in Figure 11.9. Today most lead-acid batteries are 12-V designs, assembled as six 2-V cells in series.

Each cell consists of a porous sponge lead anode and a lead dioxide cathode (usually in the form of plates) separated by porous membranes in a sulfuric acid solution. The aqueous electrolyte contains positive hydrogen and negative sulfate ions resulting from dissociation of the sulfuric acid in solution:

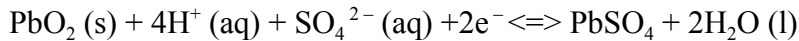


At the anode, the lead releases two electrons to the external load as it is converted to lead sulfate:

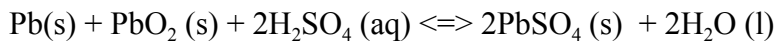


This shows that two moles of electrons are produced for each mole of sulfate ions and sponge lead reacted. Thus $j = 2$ for the lead-acid cell in Equations (11.16) and (11.17).

Meanwhile at the cathode, lead dioxide is converted to lead sulfate in the reduction reaction involving hydrogen and sulfate ions from the electrolyte and electrons from the external circuit:



The equations show that the sulfate radical (and thus sulfuric acid) is consumed at both electrodes, and that hydrogen ions combine with oxygen from the cathode material to form water that is retained in the cell. Thus the water formed as the battery discharges makes the sulfuric acid electrolyte more dilute. This is also seen in the net cell reaction, obtained as the sum of the electrode and electrolyte reactions:



It is clear that during battery discharge the lead and lead oxide electrodes are converted to lead sulfate. Furthermore, sulfuric acid is consumed and water is produced. The production of water and the consumption of sulfuric acid make the electrolyte more dilute and decrease its specific gravity. The specific gravity drops from about 1.265 when the battery is fully charged to about 1.12 when fully discharged (ref. 27). Thus the cell specific gravity is a measure of the state of discharge of the battery. A simple device called a *hydrometer*, which temporarily withdraws electrolyte from an open battery, gives a visual indication of the electrolyte specific gravity. The depth of the float in the hydrometer electrolyte indicates its specific gravity and thus the battery state of charge. When any of the reactants is depleted, the battery ceases to function. When the battery is charged by applying an external power source, the electron flow is reversed, the previously displayed reactions also reverse, and water is consumed to produce sulfate and hydrogen ions from the lead sulfate on the electrodes.

EXAMPLE 11.3

Consider the battery model of Example 11.2 for the case of 50-A current. Determine the instantaneous power output, in watts, and the rate of consumption of sulfuric acid of the cell, in kilograms per hour.

Solution

$$\text{Power} = IV = (11.1)(50) = 555 \text{ W}$$

Two moles of electrons are produced for each mole of sulfuric acid consumed at the anode. From Equation (11.16),

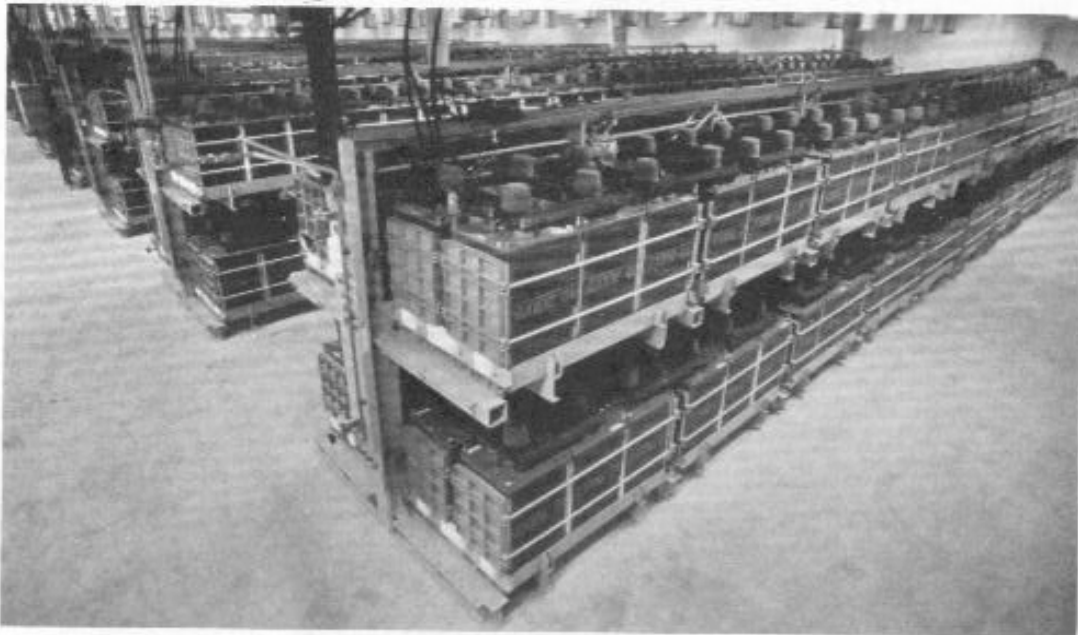


FIGURE 11.10 Lead-Acid Battery Energy Storage Facility at Chino, California. (Courtesy of Southern California Edison.)

$$n_c = I/jF = 50/(2 \cdot 96,487) = 0.000259 \text{ gm-moles/s}$$

Because sulfuric acid is consumed at the cathode at the same rate as at the anode, the total rate of acid consumption is 0.000518 gm-moles /s, or 5.18×10^{-7} kg-moles/s. The molecular weight of sulfuric acid is 98, so the mass rate of acid consumption is

$$(5.18 \times 10^{-7})(98) = 5.078 \times 10^{-5} \text{ kg/s}$$

or

$$(5.078 \times 10^{-5})(3600) = 0.1828 \text{ kg/hr}$$

Battery Applications. It is important to distinguish between SLI and traction batteries. The design of the SLI battery is governed primarily by the cranking requirements of the vehicle, usually a high current flow for a brief time interval. Once the engine is started, the alternator provides power for vehicle operating loads and to recharge the battery. During normal driving the alternator satisfies the power needs of lighting, ignition, and other electrical functions. Thus a SLI battery is usually close to fully charged and seldom deeply discharged.

The traction battery, on the other hand, usually has no energy converter available to continuously maintain the fully charged level. Thus the traction battery must be capable of operation from fully charged to almost fully discharged over a period of several hours. At least eight hours daily are normally required to return the battery to its fully charged level. This type of secondary cell is appropriate for vehicle propulsion and power plant peak-shaving applications. In the latter instance, off-peak base-load power is used to charge the battery. Later, during peak-demand periods, the battery returns a large fraction of the charging energy to the system. Such a battery is designed for thousands of charge and discharge cycles.

According to reference 4, a 10-MW, 40 MW-hr lead-acid battery storage facility was built at the Southern California Edison Company at Chino. It was designed for load-leveling use for at least 2000 deep-discharge cycles and 80% energy efficiency. Six of the cells were tested at 50°C and achieved 2300 cycles while retaining 108% of rated capacity (ref. 33). The facility, shown in Figure 11.10, uses strings of 1032 deep-discharge, 2-V lead-acid cells connected in series to provide a nominal bus voltage of 2000 V DC. A total of 8256 2-V cells, each weighing 580 pounds, are used to store 40 MW-hr for a 4-hr daily discharge cycle. A power conditioning system acts as both an inverter to provide AC output to the utility and as a rectifier to convert utility AC to DC for battery charging. The system is designed to utilize the responsiveness of battery storage to deal with wide load swings. The Chino facility is said to be able to swing from 10-MW discharge to 10-MW charge in about 16 milliseconds.

According to references 4 and 11, lead-acid batteries can now deliver energy densities of more than 40 W-h/kg. This is less than the expected performance of several other battery types. Nickel-iron batteries with an energy density of 50.4 W-hr/kg, for instance, were among 10 types endurance-tested in an electric vehicle. A van with nickel-iron batteries logged over 44,000 miles, as compared to fewer than 27,000 miles for the best performance by a lead-acid-battery-equipped van. Nickel-iron batteries, while noted for ruggedness and long life, suffer from a low energy efficiency of about 60% (ref. 34).

Space limitations allow the present discussion to only hint at the more than a century of research and the sophistication of the science and engineering of batteries.

Fuel Cells

Whereas batteries store energy in the form of chemical energy and subsequently transform it to electricity, *fuel cells* are capable of *continuous* transformation of chemical energy into electrical energy without intermediate thermal-to-mechanical conversion. Fuel cells may be thought of as chemical reactors similar to storage batteries, but with external supplies of fuel and oxidizer that react for indefinitely long time periods without substantial change in cell materials. Thus fuel cells do not run down or require recharging. As in a storage battery, reactions take place at electrodes, giving rise to a

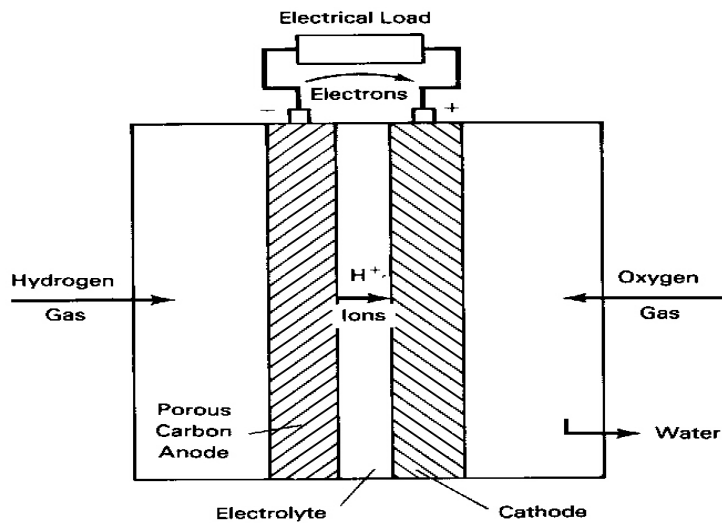


FIGURE 11.11 Schematic diagram of a hydrogen-oxygen fuel cell.

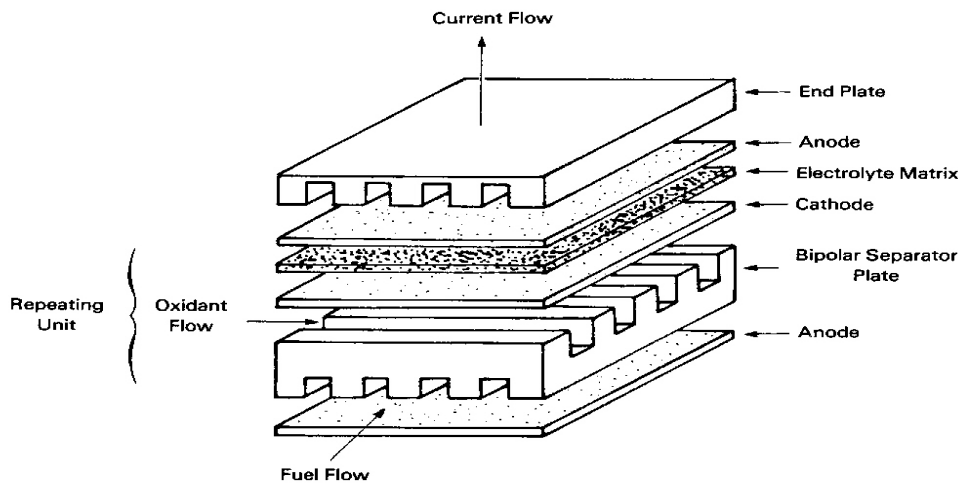


FIGURE 11.12 A basic fuel cell structure showing the repeating unit in a fuel cell stack. (Courtesy of U.S. Department of Energy, METC-88/6096.)

flow of electrons through an external circuit as depicted in Figure 11.11. An electrolyte, between the electrodes, again provides a medium for ion transfer. This allows electrons to flow through the external load while ion transport through the electrolyte maintains overall electrical neutrality of the cell.

An important element of fuel cell design is that, like large batteries, they are built from a large number of identical unit cells. Each has an open-circuit voltage on the order of one volt, depending on the oxidation-reduction reactions taking place. The fuel cells are usually built in sandwich-style assemblies called *stacks*. The schematic in Figure 11.12 shows crossflows of fuel and oxidant through a portion of a stack.

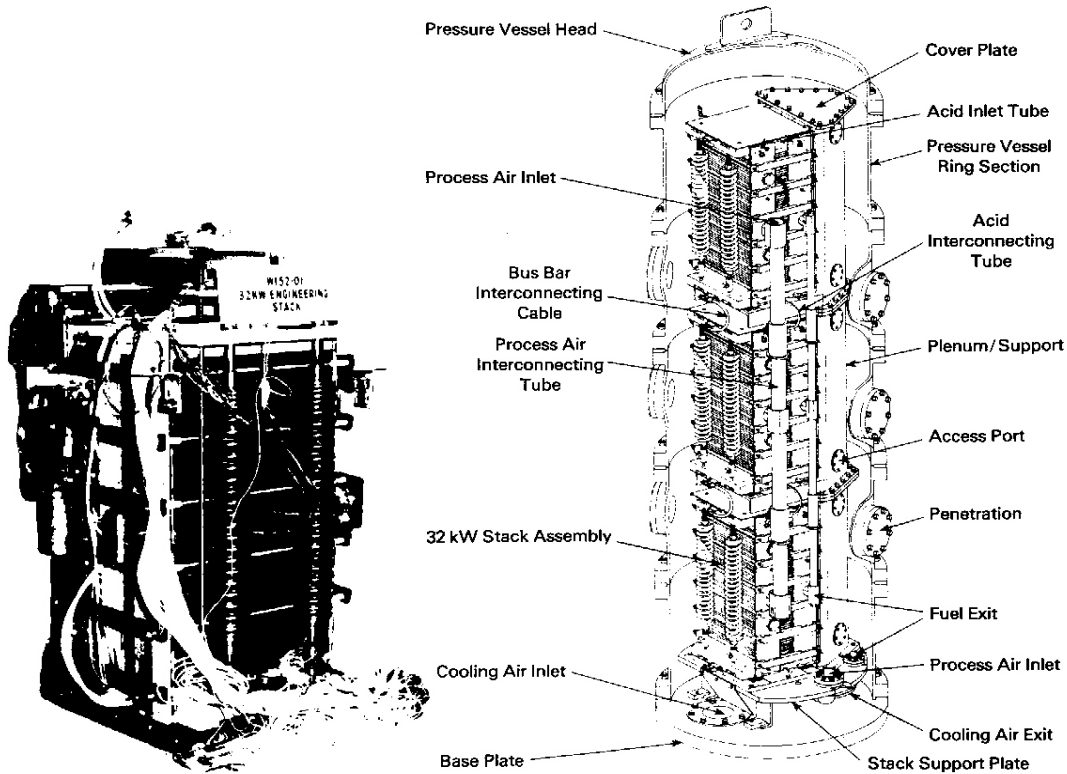


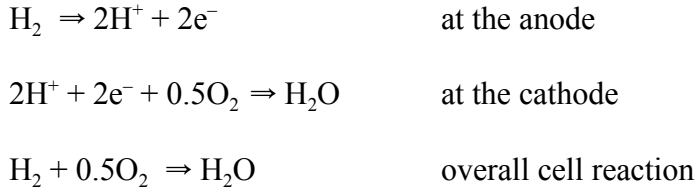
FIGURE 11.13a A 32-kW phosphoric acid fuel cell stack. (Courtesy of U.S. Department of Energy, METC-89/0266.)

FIGURE 11.13b Phosphoric acid fuel cell design made up of three 32-kW stacks. (Courtesy of U.S. Department of Energy, METC-89/0266.)

Electrically conducting bipolar separator plates serve as direct current transmission paths between successive cells. This modular type of construction allows research and development of individual cells and engineering of fuel cell systems to proceed in parallel.

A photograph of a 32-kW phosphoric acid fuel cell stack is shown in Figure 11.13(a). A conceptual design of a nominal 100-kW stack using three of the 32-kW stacks appears in Figure 11.13(b). Phosphoric acid fuel cells ideally operate with hydrogen as fuel and oxygen as oxidizer. To be economically practical in most applications, these fuel cells will probably require the use of a hydrocarbon fuel as a source of hydrogen and air as an oxidizer.

Consider the basic chemical reactions in a hydrogen-oxygen fuel cell as shown in Figure 11.11. Hydrogen molecules supplied at the anode are oxidized (lose electrons), each forming two hydrogen ions that drift through an electrolyte to the cathode. Electrons liberated from the hydrogen at the anode pass through an external circuit to the cathode, where they combine in a reduction reaction with the H^+ ions from the electrolyte and an external supply of oxygen to form water. The electrode and overall cell reaction equations are:



Thus the sole reaction product of a hydrogen–oxygen fuel cell is water, an ideal product from a pollution standpoint. In manned-space-vehicle applications the water is used for drinking and/or sanitary purposes. In addition to electrons, heat is also a reaction product. This heat must be continuously removed, as it is generated, in order to keep the cell reaction isothermal.

In the fuel cell, as in the battery, the reactions at the electrodes are surface phenomena. They occur at a liquid-solid or gas-solid interface and therefore proceed at a rate proportional to the exposed area of the solid. For this reason porous electrode materials are used, frequently porous carbon impregnated or coated with a catalyst to speed the reactions. Thus, because of microscopic pores, the electrodes effectively have a surface area many times their visible area. Any phenomenon that prevents the gas from entering the pores or deactivates the catalyst must be avoided if the cell is to function effectively over long time periods. Because of the reaction rate–area relation, fuel cell current and power output increase with increased cell area. The *power density* [W/m^2] therefore is an important parameter in comparing fuel cell designs, and the power output of a fuel cell can be scaled up by increasing its surface area.

The electrolyte acts as a medium for ion transport between electrodes. The rate of passage of positive charge through the electrolyte must match the rate of electron arrival at the opposite electrode to satisfy the physical requirement of electrical neutrality of the discharge fluids. Impediments to the rate of ion transport through the electrolyte can limit current flow and hence power output. Thus care must be taken in design to minimize the length of ion travel path and other factors that retard ion transport.

Fuel Cell Thermodynamic Analysis and Efficiencies. The theoretical maximum work of an isothermal fuel cell (or other isothermal reversible control volume) is the difference in Gibbs' function (or free energy) of the reactants (r) and the products (p). Because the enthalpy, entropy, and temperature are all thermodynamic properties, the Gibbs' function, $g = h - Ts$, is also a thermodynamic property. From the First Law, the work leaving the control volume is

$$w = h_r - h_p + q \quad [\text{J}/\text{g-mole}] \quad (11.18)$$

For a reversible isothermal process, $q = T(s_p - s_r)$, and the maximum work can be written as

$$w_{\max} = h_r - h_p + T(s_p - s_r) = g_r - g_p \quad [\text{J}/\text{g-mole}] \quad (11.19)$$

Thus the maximum work output of which a fuel cell is capable is given by the decrease in the Gibbs function.

But the maximum energy available from the fuel in an adiabatic steady-flow process is the difference in inlet and exit enthalpies, $h_r - h_p$. Defining the *fuel cell thermal efficiency* as $w_{\max}/(h_r - h_p)$, we obtain

$$\begin{aligned}\eta_{\text{th}} &= (g_r - g_p)/(h_r - h_p) \\ &= 1 - T(s_r - s_p)/(h_r - h_p) \quad \text{[dl]} \quad (11.20)\end{aligned}$$

The enthalpies and Gibbs function may be obtained from the JANAF tables for the appropriate substances (ref. 77).

EXAMPLE 11.4

Evaluate the open-circuit voltage, maximum work, and thermal efficiency for a direct hydrogen-oxygen fuel cell at the standard reference conditions for the JANAF tables. Consider the two cases when the product water is in the liquid and vapor phases.

Solution

The maximum work of the fuel cell is given by equation (11.19). The thermodynamic properties needed are obtained from the formation properties of the JANAF thermodynamic tables:

$$\begin{aligned}h_p(\text{l}) &= h_f[\text{H}_2\text{O}(\text{l})] = -285,830 \text{ kJ/kg-mole} \\ h_p(\text{g}) &= h_f[\text{H}_2\text{O}(\text{g})] = -241,826 \text{ kJ/kg-mole} \\ h_r &= h_f[\text{H}_2] + 0.5h_f[\text{O}_2] = 0.0 \text{ kJ/kg-mole} \\ g_p(\text{l}) &= g_f[\text{H}_2\text{O}(\text{l})] = -237,141 \text{ kJ/kg-mole} \\ g_p(\text{g}) &= g_f[\text{H}_2\text{O}(\text{g})] = -228,582 \text{ kJ/kg-mole} \\ g_r &= g_f[\text{H}_2] + 0.5g_f[\text{O}_2] = 0.0 \text{ kJ/kg-mole}\end{aligned}$$

Thus the maximum work for liquid-water product is:

$$w_{\max}(\text{l}) = g_r - g_p(\text{l}) = 0 - (-237,141) = 237,141 \text{ kJ/kg-mole}$$

and for water-vapor product is

$$w_{\max}(\text{g}) = g_r - g_p(\text{g}) = 0 - (-228,582) = 228,582 \text{ kJ/kg-mole}$$

of H_2 consumed or water produced in the reaction.

The theoretical ideal open-circuit voltage of the cell may also be determined from the Gibbs function using, for liquid-water product,

$$\text{EMF}(\text{l}) = w_{\max}(\text{l})/(jF) = 237,141 \times 10^3 / (2 \times 9.6487 \times 10^7) = 1.229 \text{ V}$$

For water-vapor product:

$$\text{EMF(g)} = w_{\text{max}}(\text{g}) / (jF) = 228,582 \times 10^3 / (2 \times 9.6487 \times 10^7) = 1.18 \text{ V}$$

By Equation (11.20), the thermal efficiency with liquid-water product is

$$\eta_{\text{th}}(\text{l}) = 237,141 / 285,830 = 0.8297$$

and with water-vapor product is

$$\eta_{\text{th}}(\text{g}) = 228,582 / 241,826 = 0.945$$

Regardless of the phase of the product water, a large fraction of the available enthalpy of the reactant flow is converted to work in the ideal isothermal hydrogen-oxygen fuel cell. Because the fuel cell operates as a steady-flow isothermal process and not in a cycle, the Carnot efficiency limit does not apply.

Fuel cells, like other energy conversion systems do not function in exact conformance with simplistic models or without inefficiencies. Open-circuit potentials of 0.7–0.9 volts are typical, and losses or inefficiencies in fuel cells, often called polarizations, are reflected in a cell voltage drop when the fuel cell is under load. Three major types of polarization are:

- *Ohmic Polarization*: The internal resistance to the motion of electrons through electrodes and of ions through the electrolyte.
- *Concentration Polarization*: Mass transport effects relating to diffusion of gases through porous electrodes and to the solution and dissolution of reactants and products.
- *Activation Polarization*: Related to the activation energy barriers for the various steps in the oxidation-reduction reactions at the electrodes.

The net effect of these and other polarizations is a decline in terminal voltage with increasing current drawn by the load. This voltage drop is reflected in a peak in the power-current characteristic.

The high thermal efficiencies predicted in Example 11.4 are based on operation of the fuel cell as an isothermal, steady-flow process. Although heat must be rejected, the transformation of chemical energy directly into electron flow does not rely on heat rejection in a cyclic process to a sink at low temperature as in a heat engine, which is why the Carnot efficiency limit does not apply. However, inefficiency associated with the various polarizations and incomplete fuel utilization reduce overall cell conversion efficiencies to well below the thermal efficiencies predicted in the example.

Fuel cell conversion efficiency, η_{fc} , is defined as the electrical energy output per unit mass (or mole) of fuel to the corresponding heating value of the fuel consumed. Defining the voltage efficiency, η_v , as the ratio of the terminal voltage to the theoretical EMF, V/EMF , and the current efficiency, η_i , as the ratio of the cell electrical current to the theoretical charge flow associated with the fuel consumption, we find that the conversion efficiency is related to the thermal efficiency by

$$\eta_{fc} = (V/EMF)[I/(jFn_c)]\eta_{th} = \eta_v \eta_i \eta_{th}$$

Thus the voltage efficiency accounts for the various cell polarizations previously described. Fuel cell conversion efficiencies in the range of 40–60% have been demonstrated and are possible in large-scale power plants.

EXAMPLE 11.5

The DC output voltage of a hydrogen-oxygen fuel cell with liquid-water product is 0.8 V. Assuming a current efficiency of 1, what is the fuel cell conversion efficiency?

Solution

From Example 11.4, the thermal efficiency is 0.8297 and the EMF is 1.229 V. The fuel cell conversion efficiency is then

$$\eta_{fc} = \eta_v \eta_i \eta_{th} = (0.8/1.229) \cdot 0.8297 \cdot 1.0 = 0.54$$

If heat rejected in high-temperature fuel cells is used and not wasted, overall energy efficiencies as high as 80% may be attainable. In cells that operate at high temperatures, there is an opportunity to use the thermal energy of the cell reaction products for cogeneration purposes or in a combined cycle, with a steam turbine or a gas turbine using the waste heat.

It is evident that the power output of fuel cells depends on the rate at which the reactants are consumed in the cell, just as the output of other steady-flow energy conversion systems depend on fuel and air supply rates. In low-temperature fuel cells, expensive catalysts (such as platinum) are required, to increase the rates of chemical reaction at the electrodes so that the fuel cells will be small enough to achieve reasonable power densities (per unit mass and volume).

Because chemical reaction rates increase with temperature, high-temperature fuel cells can achieve satisfactory reaction rates without catalysts or with reduced quantities. This advantage of high temperature may be offset by increased corrosion rates and other adverse effects of high temperature that reduce the fuel cell's active life. For utility applications, long, active cell life (about 40,000 hours) is considered an

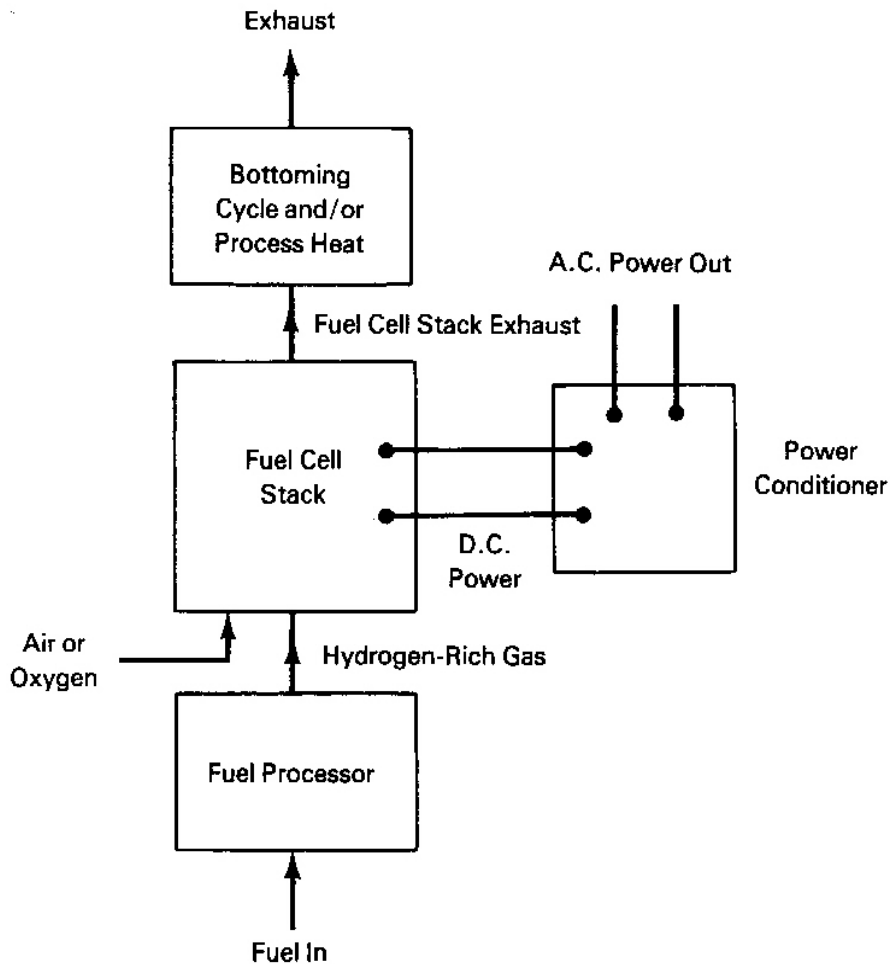
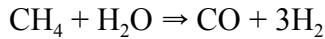


FIGURE 11.14 Schematic of a fuel cell power plant system.

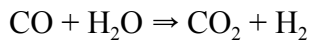
important design characteristic. It has been suggested, however, that the fuel cell stack may be a relatively small part of the cost of generation in large combined-cycle fuel cell power plants designed for long life, so that it may be acceptable to replace fuel cell stacks after shorter operating periods than other plant components, as is done with fuel rods in nuclear reactors.

While space vehicle fuel cells successfully operate on pure hydrogen and oxygen, stationary and vehicle power plants are more likely to be viable if they consume hydrocarbon fuels and air. Thus the goals of major fuel cell research and development programs focus on systems that incorporate the use of natural gas or other hydrogen-rich fuels. A utility fuel cell system appears schematically as in Figure 11.14. A fuel processor upstream of the fuel cell stack is used to prepare the incoming fuel. Its primary functions are conversion of the incoming fuel to a hydrogen-rich gas and removal of impurities such as sulphur. For natural gas, syngas, or other gaseous fuels,

the hydrocarbons may be converted by a *steam-reforming process* such as that for methane:



to produce a mixture of hydrogen and carbon monoxide. The carbon monoxide in the products can then be converted to CO_2 and produce more hydrogen in the so-called *shift reaction*:



The direct current generated by a fuel cell for utility use must be converted to alternating current by a power conditioner, as the figure suggests. High-efficiency solid, state inverters are used for this function.

Following Figure 11.14, the overall fuel cell system efficiency is then the product of a power conditioner efficiency (AC power output / DC power output), a fuel processing efficiency (enthalpy change of hydrogen / heating value of supply fuel), and the ratio of the sum of the fuel cell DC output and bottoming cycle power to the hydrogen enthalpy change.

Fuel Cell Types. Table 11.1 indicates the major fuel cell types, their convenient abbreviations, and their nominal operating temperatures. Fuel cells are usually classified according to their electrolytes, as indicated by the types in the table. While the alkaline and polymer electrolyte fuel cells were successfully demonstrated in the NASA Gemini (1-kW PEFC), Apollo (1.5-kW AFC), and Space Shuttle Orbiter (7-kW AFC) programs, these were applications with short design operating lives that used expensive catalysts to attain satisfactory reaction rates and thus may be appropriate only to space and military applications and certain limited transportation uses.

Table 11.1 Fuel Cells of Current Technical Interest

Type	Abbreviation	Operating Temperature
Polymer electrolyte fuel cell	PEFC	80°C
Alkaline fuel cell	AFC	100°C
Phosphoric acid fuel cell	PAFC	200°C
Molten carbonate fuel cell	MCFC	650°C
Solid oxide fuel cell	SOFC	1000°C

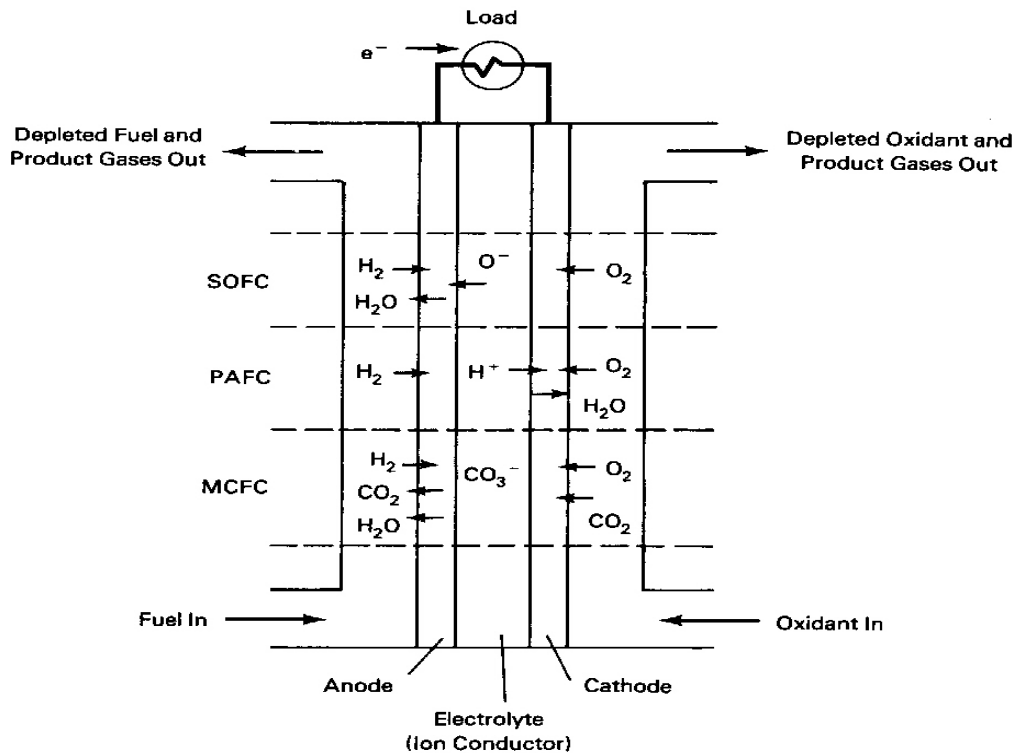


FIGURE 11.15 Schematic of a fuel cell showing the reactant/product gases and ion-conduction flow paths for PAFCs, MCFCs, and SOFCs. (Courtesy of U.S. Department of Energy, METC-88/6096.)

The last three fuel cell types listed in the table (PAFC, MCFC, and SOFC) are widely believed to be most likely to achieve commercialization for stationary power production early in the 21st century. Figure 11.15 summarizes the reactants and flow paths of these three types. The PAFC is most likely to be commercialized first, but significant progress is being made in the advanced high-temperature technologies represented by the MCFC and the SOFC.

Large-scale *phosphoric acid fuel cell* power plants have been explored based on fuel cell stacks developed by International Fuel Cells, Inc. (IFC). A basic 10-ft², 700-kW unit is shown in Figure 11.16, together with its pressure vessel. According to reference 36, The Tokyo Electric Power Company 11-MW Goi Station had twenty 700-kW fuel cell assemblies with an expected heat rate of 8300 Btu/kW-hr using liquefied natural gas as fuel.

More recently, the IFC website (ref. 81) states that the PC 25TM (a 200-kW unit) is one of five units comprising the “largest commercial fuel cell system” in the United States, which became operational in the year 2000 for the U.S. Postal Service in Anchorage, Alaska. The PC 25TM operates with hydrogen, natural gas, propane, butane, naphtha, or waste gases as its energy source. The website states that IFC delivered its 200th PC25 in the year 2000, with 3.5 million total operating hours. The PC 25 originally went into production in 1991.

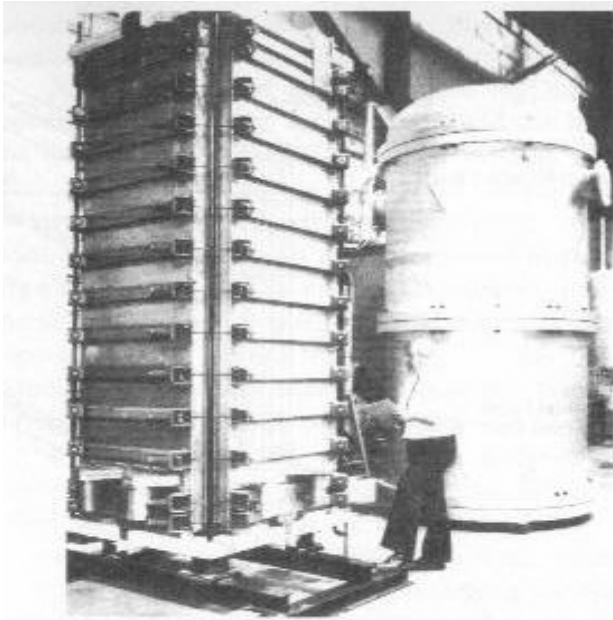


FIGURE 11.16 Ten-square-foot phosphoric acid fuel cell stack assembly for an electric utility. (Courtesy of U.S. Department of Energy, METC-89/0266.)

Reference 82 states that the ONSI Corporation (a subsidiary of IFC) PC 25 fuel cell “delivers 35 to 40 percent electrical efficiency and up to 80 percent total efficiency with heat recovery.” A 1997 DOE report (ref. 87) explores the potential for a PC 25 fuel cell cogeneration system retrofit in a large office building.

The first *molten carbonate fuel cell* power plant, a 100-kW plant operated by Pacific Gas and Electric, despite being conservatively designed for simplicity and reliability, was expected to have a heat rate of about 7000 Btu/kW-hr without a bottoming cycle. This pilot plant, located at San Ramon, Calif., uses natural gas as fuel and aimed for a cell lifetime of 25,000 hours (refs. 15 and 36). Reference 78 indicates that verification and durability testing began in June 1991 leading to a series of 2-MW demonstration plants starting in 1994, with first commercial units scheduled for 1997.

The Santa Clara Fuel Cell Demonstration project, fueled by natural gas, started construction in 1994, produced first power in March 1996, and concluded the demonstration in April 1997. Reference 84 indicates that it was “the largest and most efficient fuel cell power plant ever operated in the U.S...”

Reference 85 announces the successful completion of the grid-connected operation of a 250-kW, Fuel Cell Energy, Inc., demonstration plant as of June 2000. The plant logged more than 11,800 hours and generated more than 1.8 million kilowatt-hours of electricity. The plant is to be refitted to demonstrate a very-high-efficiency combined-cycle operation with a gas turbine.

Perhaps the most promising fuel cell type is the *solid oxide fuel cell*. The use of a solid electrolyte, as shown in Figure 11.17, allows a radical departure from the plate or sandwich type of design. The individual cells are of a closed-end cylindrical design with

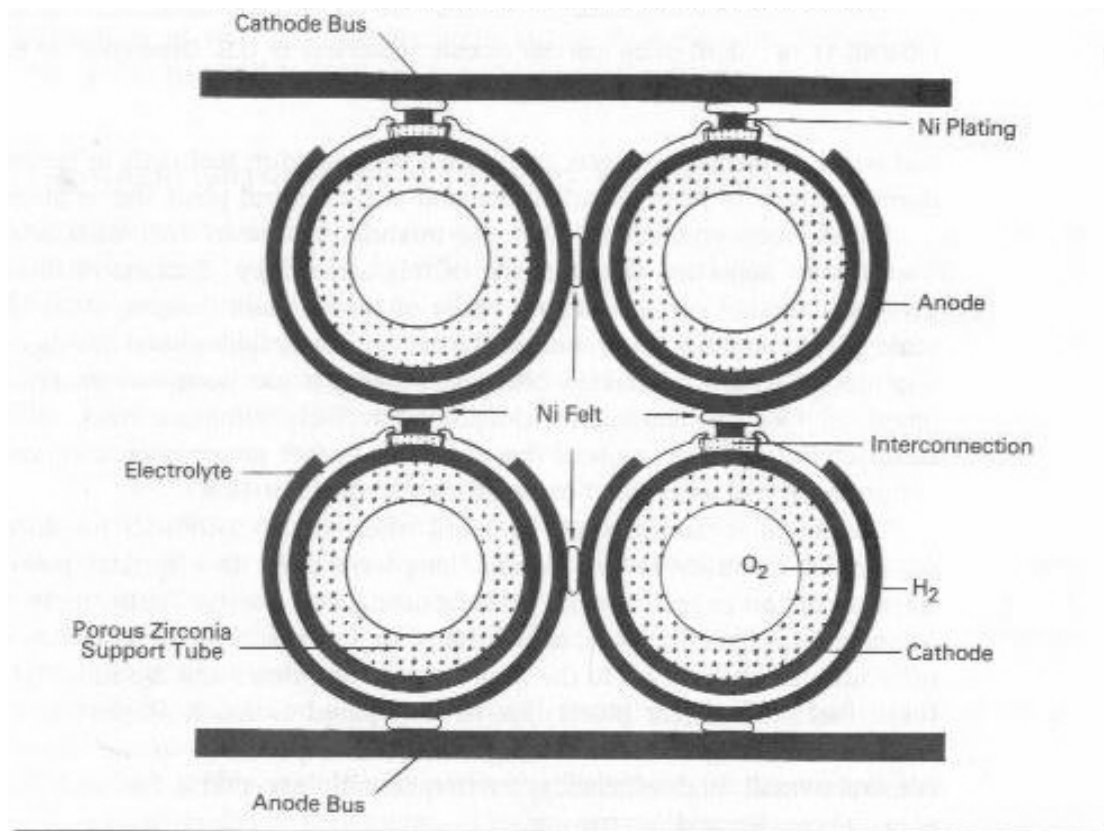


FIGURE 11.17 Cell-to-cell connections between solid oxide fuel cells. (Courtesy of U.S. Department of Energy, METC-88/6096.)

fuel manifolded to flow over the outside electrode and air on the inside communicating with the inner electrode through a porous cylindrical support structure. The clever fuel, air, and exhaust manifolding and electrical connections of this design are apparent in Figures 11.17 and 11.18. The high-temperature design allows operation without catalysts and provides an excellent opportunity to use a bottoming cycle.

Beyond high efficiency, there are several additional major characteristics of fuel cells that make them particularly attractive as energy conversion systems. First, fuel cell operation has been shown to occur with very low levels of environmental pollution (ref. 15). It has been projected that commercial fuel cells may attain pollution levels that are factors of ten below those of new conventional coal-burning power plants using the best available pollution control equipment (ref. 16).

A second important characteristic is that, because most fuel cells operate with a hydrogen-rich fuel or pure hydrogen, the fuel can be obtained from a number of sources, such as petroleum, natural gas, naphtha, methanol, and syngas made from coal. Thus a commercial stationary power plant will have a chemical processor upstream of the fuel cell stack as in Figure 11.14. The reforming and shift reactions likely to be used will produce carbon dioxide as a product. This somewhat tarnishes the environmental

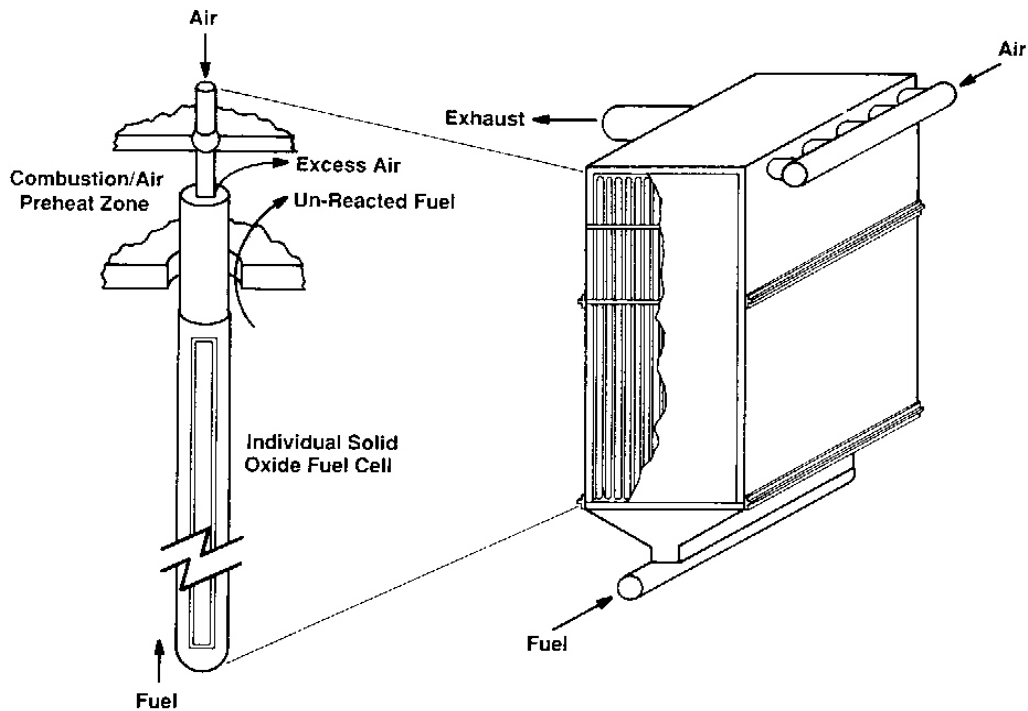


FIGURE 11.18 Solid oxide fuel cell module. (Courtesy of U.S. Department of Energy, METC-88/6096.)

beauty of the hydrogen-oxygen fuel cell concept. The chemical process to obtain hydrogen from some of the fuels may in some cases take place within the fuel cell stack.

Electrolysis of water may also be used to produce hydrogen and oxygen for fuel cell use. This provides an opportunity for energy storage by using electricity generated by base-loaded nuclear or conventional fossil fuel plants operating at off-peak hours. The hydrogen and, when appropriate, oxygen could then be reacted in fuel cells to generate electricity during periods of peak electrical demand at the central plant site or at other locations.

It has been pointed out that the modular nature of fuel cells and of fuel cell stacks is an important characteristic of this technology. Because of this modularity, a given cell design could lead to a range of power plant designs such as large utility-scale plants, smaller environmentally acceptable neighborhood plants, and industrial facilities providing combined heat and power. It has been demonstrated that scaling based on fuel cell modularity does not necessarily adversely influence stack efficiency. Their compact construction suggests that stacks and other power plant components could be factory-built and assembled in plug-in style at plant sites.

The modular nature of the fuel cell offers real possibilities for distributed power production, contrary to the historic long-term trend in electrical power production.

Because of the expected short manufacturing time for fuel cells, their apparent environmental acceptability, and their ability to function well in a variety of sizes, they offer utilities alternatives to the long construction times and the financial risks of large fossil fuel and nuclear plants that have required as much as ten years to bring into service. Thus significant advantages may be expected to accrue from the ability to construct small, high-efficiency, environmentally acceptable plants in areas where demand is growing.

While its expected high efficiency commends its use as a utility base-load plants with constant power output, the fuel cell also offers the potential for serving varying loads without substantial losses in performance. Thus fuel cells may prove useful in load-following applications as well as in base-load application.

Another potential application for fuel cells is in the large vehicle transportation sector—buses, trucks, locomotives, and the like. A likely entry for the fuel cell may be in public transportation vehicles in large cities with significant pollution problems. Reference 18 reports on studies of alternatives to battery-powered trucks in Paris, where almost 200 electric garbage trucks are currently in use. It was found that fuel-cell-powered trucks and, to a lesser degree, hybrid fuel cell/flywheel trucks (the flywheel stores extra energy for occasional vehicle accelerations while the fuel cell handles the base-load propulsion and flywheel reenergizing) would have significantly lower operating costs per ton of garbage per day than the existing battery-powered trucks. Studies also showed that diesel-powered buses were only about 10% to 20% cheaper to operate in Europe than fuel-cell-powered buses.

A simulation study, reported in reference 67, considered hypothetical fuel-cell-powered bus designs operating on three urban bus routes. A bus design specification, resulting from the study, combined two 30-kW phosphoric acid fuel cells with a 38-kW-hr battery to power a 50-kW electric traction motor. The motor transmits power to a rear wheel-axle assembly through a conventional transmission. The specification was for a 23 passenger bus for use at speeds up to 45 mph.

In April 2000, Daimler-Chrysler announced (ref. 88) an offering of 20-30 buses employing 250-kW fuel cells operating on hydrogen fuel for delivery in 2002. In these vehicles, hydrogen would be stored in eight tanks mounted on the roof over the forward axle.

These studies suggest that fuel cell technology is maturing. In many cases the economics of these systems is not yet competitive with that of existing systems. However, further advances may soon make fuel cells competitive for some transportation and stationary applications. Reference 68 gives further evidence that the quest for commercial fuel cell technology is truly international in scope.

Bibliography and References

1. Angrist, Stanley W., *Direct Energy Conversion*, 3rd ed. Newton, Mass.: Allyn & Bacon, 1976.
2. Spitzer, Lyman, *Physics of Fully Ionized Gases*, New York: Wiley-Interscience, 1956.
3. Appleby, A. J., "Advanced Fuel Cells and Their Future Market," *Ann. Rev. Energy*, 13 (1988): 267–316.
4. McLarnon, Frank R., and Cairns, Elton J., "Energy Storage," *Ann. Rev. Energy*, 14 (1989): 241–271.
5. Melde, Rolf W., "Advanced Automobile Engines For Fuel Economy, Low Emissions, and Multifuel Capability," *Ann. Rev. Energy*, 14 (1989): 425–444.
6. Jackson, John David, *Classical Electrodynamics*. New York: Wiley, 1962.
7. Fraas, Arthur P., *Engineering Evaluation of Energy Systems*. New York: McGraw-Hill, 1982.
8. Vincent, Colin A., et al., *Modern Batteries*. Baltimore: Edward Arnold, 1984.
9. Sperling, Daniel and DeLuchi, Mark A., "Transportation Energy Futures," *Ann. Rev. Energy*, 14 (1989): 375–424.
10. Fickett, A. P., "Fuel Cell Power Plants," *Scientific American*, December 1978: 70.
11. Society of Automotive Engineers, *Automotive Handbook*, 4th ed., Robert Bosch GmbH, 1996.
12. Mayfield, Manville J., Beyma, Edmund F., and Nelkin, Gary A., "Update on U.S. Department of Energy's Phosphoric Acid Fuel Cell Program." Proceedings of the Sixteenth Energy Technology Conference, February 28–March 2, 1989, Government Institutes, Inc., pp. 184–196.
13. Myles, K. M., and Krumpelt, M., "Status of Molten Carbonate Fuel Cell Technology." Proceedings of the Sixteenth Energy Technology Conference, February 28–March 2, 1989, Government Institutes, Inc., pp. 197–204.
14. Bates, J. Lambert, "Solid Oxide Fuel Cells: A Materials Challenge." Proceedings of the Sixteenth Energy Technology Conference, February 28–March 2, 1989, Government Institutes, Inc., pp. 205–219.

15. Gillis, Edward, "Fuel Cells," *EPRI Journal*, September 1989: 34–36.
16. Harder, Edwin L., *Fundamentals of Energy Production*. New York: Wiley, 1982.
17. Sissine, F., "Fuel Cells for Electric Power Production: Future Potential, Federal Role and Policy Options," in *Fuel Cells: Trends In Research and Applications*, Ed. A. J. Appleby. Washington: Hemisphere, 1987.
18. Appleby, A. J., "Phosphoric Acid Fuel Cells," in *Fuel Cells: Trends In Research and Applications*, Ed. A. J. Appleby. Washington: Hemisphere, 1987.
19. Appleby, A. J. (Ed.), *Fuel Cells: Trends In Research and Applications*, Washington: Hemisphere, 1987.
20. Ketelaar, J. A. A., "Molten Carbonate Fuel Cells," *Fuel Cells: Trends In Research and Applications*, Ed. A. J. Appleby. Washington: Hemisphere, 1987.
21. Kinoshita, K., McLarnon, R. R., and Cairns, E.J., *Fuel Cells: A Handbook.*, U.S. Department of Energy METC-88/6096, 1988.
22. Berry, D.A., and Mayfield, M.J., *Fuel Cells, Technology Status Report*, U.S. Department of Energy METC-89/0266, 1988.
23. Anon., *Fuel Cell Systems Program Plan, FY 1990*, U.S. Department of Energy, FE-0106P, October 1989.
24. Huber, W. J., *Proceedings of the First Annual Fuel Cells Contractors Review Meeting*, U.S. Department of Energy METC-89/6105, May 1989.
25. Anon., *1988 Fuel Cell Seminar*. Washington, D.C.: Courtesy Associates, 1988.
26. Feynman, Richard P., Leighton, Robert B. and Sands, Matthew, *The Feynman Lectures on Physics*, Vol. 2. Reading, Mass.: Addison-Wesley, 1964.
27. Anon., *Battery Service Manual*. Chicago: Battery Council International, 1987.
28. Kotz, John C., and Purcell, Keith F., *Chemistry and Chemical Reactivity*. Philadelphia: Saunders, 1987.
29. Goodman, Frank, "Power Electronics for Renewables," *EPRI Journal*, January/February 1988: 44–47.

30. Schaefer, John, "Photovoltaic Operating Experience," *EPRI Journal*, March 1988: 40–42.
31. Peterson, Terry, "Amorphous Silicon Thin Film Solar Cells," *EPRI Journal*, June 1988: 41–44.
32. Dostalek, Frank, "High Concentration Photovoltaics," *EPRI Journal*, March 1989: 46–49.
33. Morris, Douglas, "The Chino Battery Facility," *EPRI Journal*, March 1988: 46–50.
34. Purcell, Gary, and Driggans, Rick, "Electric Vehicle Testing at TVA," *EPRI Journal*, March 1988: 44–46.
35. Anon., *The Storage Battery*. Horsham, Pa.: Exide Corp., 1980.
36. Makanski, Jason, "Fuel Cells Extend Boundaries of Process/Power Integration," *Power*, May 1990: 82–86.
37. Chapman, Alan J., *Heat Transfer*, New York: Macmillan, 1968.
38. Swanson, Theodore D., "Large Scale Photovoltaic System Design Considerations," *The Handbook of Photovoltaic Applications*. Atlanta, Ga.: Fairmont Press, 1986, pp. 19–32.
39. Van Overstraeten, R.J., and Mertens, R.P., *Physics, Technology, and Use of Photovoltaics*. Boston: Adam Hilger, 1986.
40. McDaniels, David K., *The Sun: Our Future Energy Source*, 2nd ed. New York: Wiley, 1984.
41. Feynman, Richard P., Leighton, Robert B. and Sands, Matthew, *The Feynman Lectures on Physics*, Vol. 3, Reading, Mass.: Addison-Wesley, 1965.
42. Takahashi, K. and Konagai, M., *Amorphous Silicon Solar Cells*. New York: Wiley, 1986.
43. Duffie, John A., and Beckman, William A., *Solar Engineering of Thermal Processes*. New York: Wiley, 1980.
44. Rosa, Richard J., *Magnetohydrodynamic Energy Conversion*, rev. ed. Washington: Hemisphere, 1987.

45. Gregory, Derek P., "The Hydrogen Economy," *Scientific American*, Vol. 228, No.1, (January 1973) 13–21.
46. Gregory, D. P. and Pangborn, J.B., "Hydrogen Energy", *Ann. Rev. Energy*, 1 (1976): 279–310.
47. Cogineni, M. Rao, Andrus, H.E. Jr., and Jones, T.J., "Advanced Energy Systems." Proceedings of the American Power Conference, Vol. 50, 1988, pp. 282–287.
48. Bajura, R. A., and Halow, J.S., " Looking Beyond the Demonstration Plants: Longer-Term, Coal-Based Technology Options." Proceedings of the American Power Conference, Vol. 50, 1988, pp. 49–56.
49. DeMeo, Edgar, et al., "Thin Films: Expanding the Solar Marketplace", *EPRI Journal*, March 1989: 4–15.
50. Wood, Bernard W., *Applications of Thermodynamics*, 2nd ed. Reading, Mass.: Addison-Wesley, 1982.
51. Womack, G. J., *MHD Power Generation: Engineering Aspects*. London: Chapman and Hall, 1969.
52. Soo, S. L., *Direct Energy Conversion*. Engelwood Cliffs, N.J.: Prentice Hall, 1968.
53. Kettani, M. Ali, *Direct Energy Conversion*. Reading, Mass.: Addison Wesley, 1970.
54. Sutton, George W., *Direct Energy Conversion*. New York: McGraw-Hill, 1966.
55. Pitts, Donald R., and Sissom, Leighton E., *Heat Transfer*, Shaum's Outline Series. New York: McGraw-Hill, 1977.
56. Anon., *The Astronomical Almanac*. Washington, D.C.: U. S. Government Printing Office, 1990.
57. Parsons, Robert A. (Ed.), *The ASHRAE Handbook*, HVAC Systems and Applications Volume. Atlanta, Ga.: American Society of Heating, Refrigerating, and Air Conditioning Engineers, 1987.
58. DeMeo, Edgar, "Getting Down to Business with Thin Films," *EPRI Journal*, March 1989: 4–15.

59. Taylor, Roger W., Cummings, John E., and Swanson, Richard M., "High Efficiency Photovoltaic Device Development: An Example of the R&D Process" Proceedings of the American Power Conference, Vol. 47, 1985, pp. 255–259.
60. Bockris, J. O. M., *Energy The Solar-Hydrogen Alternative*. New York: Wiley, 1975.
61. Williams, L. O., *Hydrogen Power*, Elmsford, N. Y.: Pergamon Press, 1980.
62. Sze, S. M., *Semiconductor Devices Physics and Technology*. New York: Wiley, 1985.
63. Moore, Taylor, et al., "Opening the Door for Utility Photovoltaics," *EPRI Journal*, January–February 1987: 5–15.
64. Griffiths, David, J., *Introduction to Electrodynamics*, 2nd ed. Engelwood Cliffs, N. J.: Prentice-Hall, 1989.
65. Anon., "Solar Electric Generating Stations (SEGS)," *IEEE Power Engineering Review*, August, 1989: 4–8.
66. Anon., "Promise of Solar Energy Being Fulfilled in California," *Power*, October 1989: s32—s36.
67. Romano, Samuel, "Fuel Cells for Transportation," *Mechanical Engineering*, August 1989: 74–77.
68. Hirschenhofer, J. H., "International Developments in Fuel Cells," *Mechanical Engineering*, August 1989: 78–83.
69. Carlson, D. E., "Photovoltaic Technologies for Commercial Power Generation," *Annual Review of Energy*, Vol. 15, 1990, pp. 85–98.
70. MacDonald, Gordon J., "The Future of Methane as an Energy Resource," *Annual Review of Energy*, Vol. 15, 1990, pp. 53–83.
71. Moore, Taylor, et al., "On-Site Utility Applications for Photovoltaics," *EPRI Journal*, March 1991: 26–37.
72. Moore, Taylor, et al., "Thin Films: Expanding the Solar Marketplace," *EPRI Journal*, March 1989: 4–15.

73. Smock, Robert W., "Second Generation Fuel Cell Technology Moves Toward Demos," *Power Engineering*, June 1990: 10.
74. Sapre, Alex R., "Properties, Performance and Emissions of Medium-Concentration Methanol-Gasoline Blends in a Single-Cylinder, Spark-Ignition Engine," SAE Paper 881679, October 1988.
75. Douglas, John, "Beyond Steam: Breaking Through Performance Limits," *EPRI Journal*, December 1990: 5–11.
76. Graff, Eric, Texas Instruments Co. Personal Communication, May 24, 1991.
77. Chase, M. W. Jr., et al., *JANAF Thermodynamic Tables*, 3rd ed., *J. Phys. Chem. Ref. Data* 14, Supplement No. 1, 1985.
78. Douglas, John, et al., "Fuel Cells for Urban Power," *EPRI Journal*, September 1991: 5–11.
79. Howell, John R., Bannerot, Richard B., and Vliet, Gary C., *Solar-Thermal Energy Systems*. New York: McGraw-Hill, 1982.
80. Levine, Jules D., et al., "Basic Properties of the Spherical Solar Cell." 22nd Photovoltaic Specialists Conference, Las Vegas, Nev., 1991.
81. International Fuel Cells: Clean, Reliable Fuel Cell Energy, www.internationalfuelcells.com/index_fl1.shtml, (November 14, 2000)
82. Rulseh, Ted, "Fuel Cells: From Promise to Performance," *Grid*, Spring/Summer 2000: 15.
83. Santa Clara Demonstration Project, www.ttcorp.com/fccg/scdpnew1.htm, (November 14, 2000)
84. Fuel Cell Energy, Carbonate Fuel Cell Manufacturer, www.ttcorp.com/fccg/erc_abt.htm, (November 15, 2000)
85. Welcome to Fuel Cell Energy, Inc., www.fuelcellenergy.com/, What's New?, (November 15, 2000)
86. Library of Fuel Cell Related Publications, <http://216.51.18.233/biblio.html>, (November 14, 2000)

87. Archer, David H., and Wimer, John G., “ A Phosphoric Acid Fuel Cell Cogeneration System Retrofit to a Large Office Building,” Department of Energy FETC-97/1044, April 1997., www.fetc.doe.gov/netltv/index.html, (November 15, 2000)

88. DaimlerChrysler Offers First Commercial Fuel Cell Buses to Transit Agencies, www.hfcletter.com/letter/may00/feature.html, (November 15, 2000)

EXERCISES

- 11.1* Derive an expression for the battery power output, in terms of E and R_i/R_o , for the linear model discussed in connection with Example 11.2. Nondimensionalize the power by dividing by E^2/R_o . Use a spreadsheet to tabulate and plot the dimensionless power as a function of R_i/R_o .
- 11.2* Derive an expression for the linear-battery-model power output nondimensionalized by E^2/R_i in terms of the internal-to-external resistance ratio. Use a spreadsheet to tabulate the dimensionless power function, and plot it. Is there a condition that produces an extreme value of the dimensionless power? If so, use calculus methods to derive the condition.
- 11.3 An automobile storage battery with an open-circuit voltage of 12.8V is rated at 260 A-hr. The internal resistance of the battery is 0.2Ω . Estimate the maximum duration of current flow and its value through an external resistance of 1.8Ω .
- 11.4 A battery electrical storage plant is to be designed for 20-MW peak power delivery for a duration of four hours. The plant uses 600 A-hr batteries operating at 400 volts DC. Estimate the minimum number of batteries and the current in each during peak operation.
- 11.5 A hydrogen-oxygen fuel cell operates with a voltage of 0.7v with water-vapor product. Calculate the work per kg-mole of hydrogen, in kJ and in kW-hr, and determine the cell efficiency.
- 11.6 A neighborhood fuel cell power plant is to be designed for an electrical power output of 2000 kW with liquid-water product. Estimate the flow rates of hydrogen and oxygen during peak power production, assuming that an 80% efficient power conditioner is used to convert DC to AC power and that the fuel cell efficiency is 55%. What is the plant heat rate?

* Exercise numbers with an asterisk involve computer usage.

- 11.7 A hydrogen-oxygen fuel cell has liquid water as product when it operates at 0.82 volts. What is the electrical energy output, in kJ / kg-mole of hydrogen, and the cell efficiency?
- 11.8 Prepare a typed three-page, double-spaced memorandum outlining the design of the power train of a hydrogen-oxygen fuel-cell-powered automobile, giving the design criteria, system description, and quantitative preliminary design data on the power and fuel supply systems.
- 11.9 A hydrogen-oxygen fuel cell stack produces 50 kW of DC power at an efficiency of 60%, with water-vapor as product. What is the hydrogen mass flow rate, in g/s, and the cell voltage?
- 11.10 A fuel cell power plant is to be designed for an electrical power output of 200-MW with liquid-water product. Estimate the flow rates of hydrogen and oxygen during peak power production with an 85% efficient power conditioner and fuel cell efficiency of 55%. What is the plant heat rate?